Far-infrared laser spectroscopy of the linear Ising system $CoCl_2 \cdot 2H_2O$†

D. F. Nicoli* and M. Tinkham

Department of Physics and Division of Engineering and Applied Physics, Harvard University, Cambridge, Massachusetts 02138

(Received 30 July 1973)

The far-infrared transmission of the linear-chain magnetic insulator $CoCl_2 \cdot 2H_2O$ (CC2) has been measured with high resolution at the HCN/DCN laser frequencies of 29.7, 32.2, 51.4, and 52.7 cm^{-1}. The spin-cluster excitations observed by Torrance and Tinkham in this nearly Ising $S = 1/2$ system have been studied in detail in magnetic fields up to 120 kOe, particularly the temperature dependence of the linewidths and intensities in the range 1.3–15 °K. "Multimagnons" which flip up to 14 adjacent spins, with corresponding g values as high as $14 \times 6.8 \simeq 95$, have been observed. The existence of an optic phonon at 29 cm^{-1}, strongly coupled to the "spin-wave" excitation, was verified using the deuterated form of CC2. Additional weak resonances have been seen in the antiferromagnetic and ferrimagnetic phases; these have been identified as spin clusters associated with domain walls, as recently postulated by Motokawa. The intrinsic multimagnon line shapes are highly Lorentzian; observed asymmetries are due almost entirely to dimensional interference effects. The relative spin-cluster intensities agree with theoretical values obtained from the eigenvectors of the CC2 single-chain Hamiltonian. The linewidths Γ of those clusters which can be measured over a substantial temperature range follow the universal form $\Gamma(T) \simeq \Gamma_0 + Ae^{-\Delta/kT}$, with $\Delta/k \simeq 43$ °K (30 cm^{-1}); at a given elevated temperature the linewidth increases dramatically with increasing cluster size. Possible mechanisms are briefly discussed. The integrated intensities fall off slowly with increasing temperature, obeying statistical predictions of the ideal Ising chain. This work supports the spectroscopic value of intrachain exchange, $J_0^{zz} \simeq 12.7$ cm^{-1}, which is roughly twice the size of indirect estimates based on mean-field calculations.

I. INTRODUCTION

$CoCl_2 \cdot 2H_2O$, or CC2, is a linear-chain magnetic insulator.[1–14] At low temperatures ($T_N \approx 17$ °K) it can be magnetically described as consisting of $S = \frac{1}{2}$ spins which are strongly ferromagnetically bound to form chains; these chains, in turn, are relatively weakly coupled to each other. For $T \ll T_N$, the stable ordering of these chains is as follows: antiferromagnetic (AF) below $H_{c1} \approx 31$ kOe; ferrimagnetic (Fi) between H_{c1} and $H_{c2} \approx 45$ kOe; and ferromagnetic (Fo) above H_{c2}. The transitions at H_{c1} and H_{c2} are metamagnetic owing to the large anisotropy of the interchain exchange field. The excitation spectrum of CC2 was investigated in the microwave regime by Date and Motokawa[15–17] and in the far infrared by Torrance and Tinkham.[18–21] The latter authors used a mercury-arc grating-monochromator source to cover the range 20–60 cm^{-1}, with applied fields of 0 to 55 kOe. Their spectroscopy for the most part was performed at 1.6 °K.

The work reported here[22–24] utilized monochromatic radiation from an HCN/DCN laser, thereby allowing a much higher resolution study of the CC2 spectrum. The central position of the laser lines relative to the Torrance-Tinkham spectrum is shown in Fig. 1. The molecular laser source offers to the far infrared the great advantages paralleled in the microwave regime by the klystron. The new level of information which can be obtained from magnetic spectra include accurate measurement of linewidths and absolute intensities as well as the resolution in field of very weak excitations.

A cursory reading of Fig. 1 reveals a basic *fan* structure of excitations, occurring once for each sublattice of the three distinct phases. Such a structure was recognized to closely resemble the excitation spectrum of the linear Ising model,

$$E_n = 2J_0^{zz} + ng^{\parallel}\mu_B H, \tag{1}$$

where J_0^{zz} is the *intra*chain exchange and $g^{\parallel}(\equiv g^{zz})$ is the (longitudinal) effective g factor. In the localized spin-flip picture the lowest excited states correspond to the creation of single "spin clusters" containing an arbitrary number of *adjacent* flipped spins.

The presumption of Torrance and Tinkham, therefore, was that an excellent basis choice for the diagonalization of the general spin-exchange Hamiltonian for a single chain should be the eigenfunctions of the Ising chain. These are the so-called Ising basis functions (IBF's):

$$|n; K\rangle = \frac{1}{\sqrt{N}} \sum_i^N e^{iKR_i} S_i^- S_{i+1}^- \cdots S_{i+n-1}^- |0\rangle, \tag{2}$$

where n is the size of the spin cluster, K is the momentum of the propagating cluster, R_i is the coordinate of the cluster center (arbitrary zero), and $|0\rangle$ represents the (normalized) fully aligned chain of N spins (N large)—all spins "up."

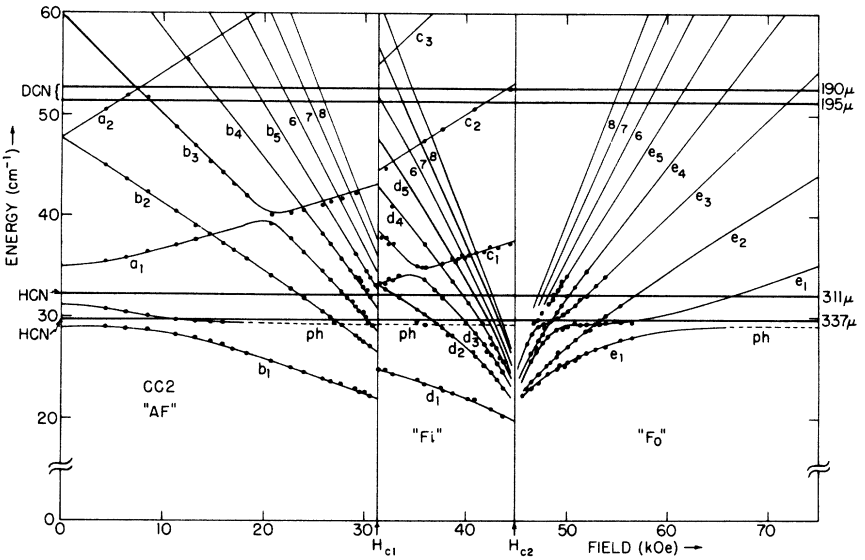

FIG. 1. Theoretical E-vs-H spectrum of CC2 according to Torrance and Tinkham, showing excellent agreement with their experimental data points of 1.6 and 6 °K. The HCN and DCN laser frequencies are shown superimposed on this plot.

The general nearest-neighbor single-chain Hamiltonian can be written

$$\mathcal{H} = \mathcal{H}^{\text{Ising}} + \mathcal{H}^{\perp} + \mathcal{H}^{a}, \tag{3a}$$

where

$$\mathcal{H}^{\text{Ising}} \equiv -\sum_{i}^{N} (2J_0^{zz} S_i^z S_{i+1}^z + g^{\parallel}\mu_B H S_i^z), \tag{3b}$$

$$\mathcal{H}^{\perp} \equiv -\sum_{i}^{N} J_0^{\perp}(S_i^+ S_{i+1}^- + \text{H. c.});$$

$$J_0^{\perp} \equiv \tfrac{1}{2}(J_0^{xx} + J_0^{yy}), \tag{3c}$$

$$\mathcal{H}^{a} \equiv -\sum_{i}^{N} J_0^{a}(S_i^+ S_{i+1}^+ + \text{H. c.});$$

$$J_0^{a} \equiv \tfrac{1}{2}\left| J_0^{xx} - J_0^{yy} \right|. \tag{3d}$$

The approximate diagonalization of $\mathcal{H}$ was performed using the states $|n; K=0\rangle \equiv |n\rangle$ of Eq. (2). Also, Torrance and Tinkham postulated the existence of an optic phonon at 29.3 cm^{-1} to account for the bending and splitting of the $n=1$ clusters (ordinary spin waves). The striking quantitative fit to the data seen in Fig. 1 permitted the unambiguous determination of J_0 and g^{zz} ($J_0^{zz} = 12.7$ cm^{-1}; $g^{zz} = 6.8$) as well as good estimates for $J_0^{\perp}$, J_0^{a}, and the *inter*chain exchange values.

The three phase configurations for CC2 are shown in Fig. 2, along with the labeling conventions for interchain exchanges J_1 and J_2. The spin-cluster excitations in the fully aligned Fo phase are labeled e_n, where n denotes the cluster size. Excitation e_1 is equivalent to the ordinary ferromagnetic spin wave.

CC2 has been recognized to be a rather special magnetic material. It is a linear-chain system, with *intra*chain exchange much stronger than the *inter*chain values, allowing one to focus on an isolated chain. Its highly uniaxial exchange yields approximately one-dimensional Ising behavior; the spin-cluster excitations actually exist as bound states, considerably separated in energy from the two-magnon continuum. Furthermore, it is only the existence of a large transverse anisotropy in intrachain exchange J_0^{a} which allows spin clusters of size larger than $n=1$ to be excited from the ground state with observable intensities, owing to a coupling by $\mathcal{H}^{a}$;

$$\langle n; K | \mathcal{H}^{a} | n \pm 2; K \rangle = -2J_0^{a}. \tag{4}$$

Hence, the states corresponding to $n=1$, 3, 5, 7, etc., become admixed and form the "odd manifold" of states, accessible from the ground state via transversely polarized radiation. The states corresponding to $n=2$, 4, 6, 8, etc., are coupled to each other (and to the fully aligned state $|0\rangle$) to form the "even manifold" of states, accessible from the ground state via parallel polarized radiation.

II. EXPERIMENTAL SYSTEM

The experiments consisted of measuring the transmission of far-infrared laser radiation through millimeter-thick aligned slabs of single crystal $CoCl_2 \cdot 2H_2O$ (CC2) and $CoCl_2 \cdot 2D_2O$ (CC2D) as a function of slow-swept magnetic field. The field range covered was 0 to approximately 125 kOe, with sample temperature adjustable between 1.3 and 18 °K. The laser frequencies utilized were the two strong HCN lines at 29.7 and 32.2 cm^{-1}, as well as the DCN pair at 51.4 and 52.7 cm^{-1}. Details of the apparatus design including the laser-output feedback stabilizer are reported elsewhere.[22,23,25]

A precision crystal-slicing jig was constructed

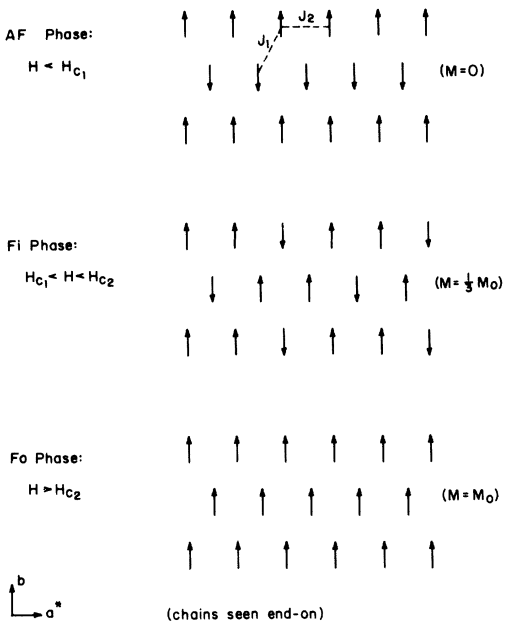

FIG. 2. Three magnetic phases of CC2 for $T \ll T_N$ ($\cong 17\,^\circ$K). Each spin represents a ferromagnetic linear chain which runs normal to the plane of the figure.

to facilitate preparation of CC2 sample slabs containing the (100), or b-c, plane. With the external field applied along the "easy" b axis and the radiation incident normal to the b-c plane, two polarization choices permit complete separation of the two cluster manifolds: h_{osc} parallel and perpendicular to the b axis, exciting even and odd n, respectively. GE No. 7031 varnish was used to mount and seal the samples. The radiation aperture at the sample was chosen to be a circle only 2.5 mm in diameter to avoid possible line broadening due to field inhomogeneity. Signal levels as high as several mV from the Ga-doped-Ge bolometer detector were obtained from 1.0-mm-thick samples and the strong 29.7-cm^{-1} laser line.

The laser cavity is of plano/concave design, containing two 10-cm-diameter mirrors, spaced 2.3 m apart. The fixed mirror is flat, with an 8-mm output coupling hole for HCN operation and a 2-mm hole for DCN (lower gain). The translatable mirror is concave with a 10-m radius of curvature.

The dc plasma discharge is obtained with either a hot or water-cooled cathode. The former was most often used, and consisted of a large neon-sign electrode (No. 19CC) run at a current of 750–800 mA. Its lifetime is only between 3 and 6 h at this high current, but the resulting laser output is quiet to a few parts in 10^4, short term, given stable gas flow and active current regulation. The starting gases used in the flowthrough system are NH_3 and CH_4 in roughly equal proportions for HCN operation and deuterated acetonitrile vapor (CD_3CN) for DCN. The typical operating voltage is 1100–1400 V, with a running series ballast of about 900 Ω; the familiar striated-glow plasma results. A fast-slewing programmable power supply (Kepco JQE 100-MHS) is used to provide discharge current regulation at the 0.1% level or better.

An output power stabilization control was designed to deal with the slow drifts induced by thermal expansion of cavity components. Power output is monitored by a thermostated TGS pyroelectric detector, which adjusts the laser mirror separation by means of a 2000-V programmable power supply and a sensitive (0.75 μm/100 V) PZT piezoelectric transducer.[25] Output power stability of 1% or better over the long term is easily achieved.

III. EXPERIMENTAL RESULTS—E vs H SPECTRUM AT LOW T

A. Quality of spectra observed

Figures 3(a) and 3(b) contain representative spectra obtained from field sweeps at 29.7 cm^{-1} with the two polarizations appropriate to even- and odd-manifold excitation. The most exciting feature

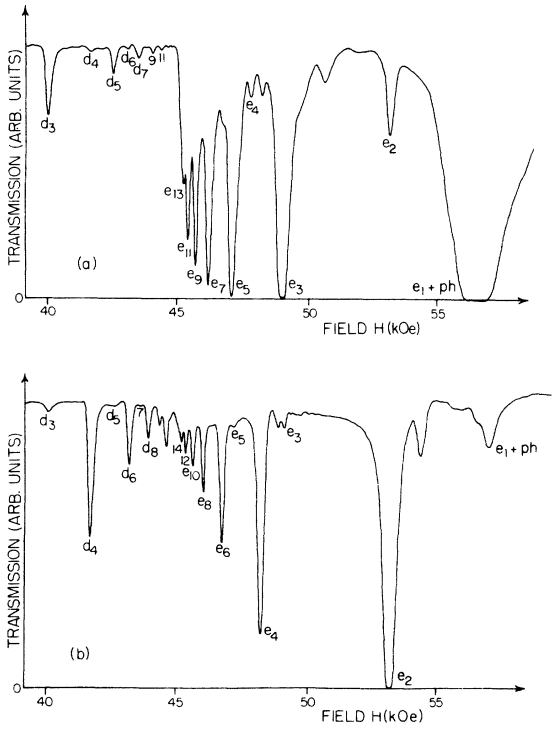

FIG. 3. Representative 29.7-cm^{-1} laser transmission spectra of CC2 at 1.3 °K in the Fi and Fo phases for two polarizations: (a) perpendicular ($H_{osc} \perp b$), and (b) parallel ($H_{osc} \parallel b$).

of these laser spectra is the clear presence of the creation of *very large* spin clusters—indeed, of up to 14 adjacent flipped spins. The effective g factor for such a "multimagnon" is $14\times6.8=95$! Torrance and Tinkham were barely able to discern the $n=5$ cluster in the Fo region, owing to the extremely low intensity and substantial energy impurity of the monochromator (almost 1-cm^{-1} energy width from the finite slit sizes plus some harmonic content which escapes crystal filtering). One must compare typical laser spectra to the best monochromator data to appreciate the significance of this advance in the spectroscopy. As can be seen in the representative sweeps [especially Fig. 3(a)], the present limitation against the observation of resonances corresponding to even larger size clusters (very near H_{c2}) lies more with the merging of these magnons owing to finite widths and decreasing field separation than with insufficient intensity. It can be seen from these sample spectra that some of the stronger resonances possess asymmetric line shapes. The mechanism responsible for these shapes will be discussed later. The $n=1$ (spin-wave) and $n=2$ clusters in all three phases are strong enough to cause the transmission to be effectively zero on a linear scale over a finite field range about the resonance peak for 1-mm-thick crystals. CC2 is sufficiently brittle that it is difficult to slice crystals thinner than about 0.5–0.6 mm. As closely as can be discerned, the bottoming levels correspond to true zero transmission.

Field sweeps like those of Figs. 3(a) and 3(b) all exhibit a common feature: Spin clusters belonging to the "wrong" polarization are present. They appear at their expected field locations but have only 1 to 10% of the strength they would normally possess using the correct polarization. The presence of the "wrong" manifold of lines appears to be due entirely to imperfect sample-polarizer alignment with respect to the applied field rather than a genuine selection rule breakdown [i.e., Hamiltonian different from Eq. (3a)]. In the authors' cryostat, rotations of both the sample holder and polarizer can be performed in only *one* plane–the b-c. From alignment optimization it was concluded that the remnant intensity exists as a consequence of imperfect sample alignment in the a-b plane (owing to holder tilt, slicing errors, and nonuniform gluing), over which we had *no* control while taking data. Hence, typically no great effort was expended to extinguish the "wrong" lines. One can easily estimate the modification to the Ising excitation spectrum owing to a small misalignment of the applied field with respect to the easy b axis. Both the exchange energy intercept and the magnon slopes are reduced in size, by approximately the cosine of the misalignment angle. For misalignment angles of less than 10° the resulting shifts in laser intersection fields are essentially negligible.

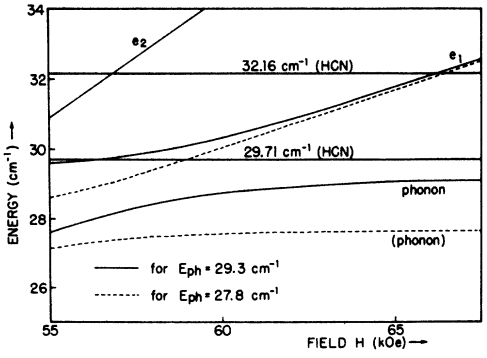

FIG. 4. Detailed view of the theoretical E-vs-H spectrum of CC2, Fo phase, expected for two different phonon energies. The 27.8-cm^{-1} value has been postulated for the deuterated crystal $CoCl_2\cdot2D_2O$.

B. Optic phonon verification

The Torrance-Tinkham spectrum revealed a bending and splitting of spin waves b_1 and e_1 (and also of the higher e_{odd} due to their strong coupling to e_1 near 30 cm^{-1}) that implied the existence of a field-independent level at approximately 29 cm^{-1}. In the Hamiltonian diagonalization the presumed phonon was added to the set of $K=0$ spin-cluster basis states; the excellent fit seen in Fig. 1 was obtained using the following parameters: phonon energy $(E_{ph})=29.3$ cm^{-1} and $(n=1)$ magnon-phonon coupling $(A_{ph})=0.55$ cm^{-1}, AF phase, and $\sqrt{2}\times0.55$ cm^{-1}, Fo phase. (There is no d_1 or c_1 crossing in the Fi phase to determine A_{ph} there. The origin of the $\sqrt{2}$ factor is explained in Ref. 26.)

The obvious experiment was performed–CC2D crystals were grown, thereby increasing the water mass by 11%. The anticipated phonon frequency for CC2D, assuming oscillation of the entire water mass as a unit and ignoring the small reduced-mass correction due to the finite heavier ion masses, is

$$E_{ph}(\mathrm{CC2D})\cong[M(H_2O)/M(D_2O)]^{1/2}\times29.3\ \mathrm{cm}^{-1}$$
$$\cong27.8\ \mathrm{cm}^{-1},$$

or a 5% decrease in frequency. Since the lower HCN laser line is barely 0.4 cm^{-1} above the frequency claimed for the CC2 optic phonon, the field intersections of b_1+phonon and e_1+phonon with it are highly sensitive to small changes in E_{ph}.

Figure 4 contains the relevant portion of the Fo-phase excitation spectrum obtained from the diagonalization, showing the e_1+phonon level for the two phonon energies. The magnon-phonon coupling strength A_{ph} is assumed not to vary with deuteration; also, the constancy of transition field H_{c1} and H_{c2} (at low T) is presumed. The shift in the e_1

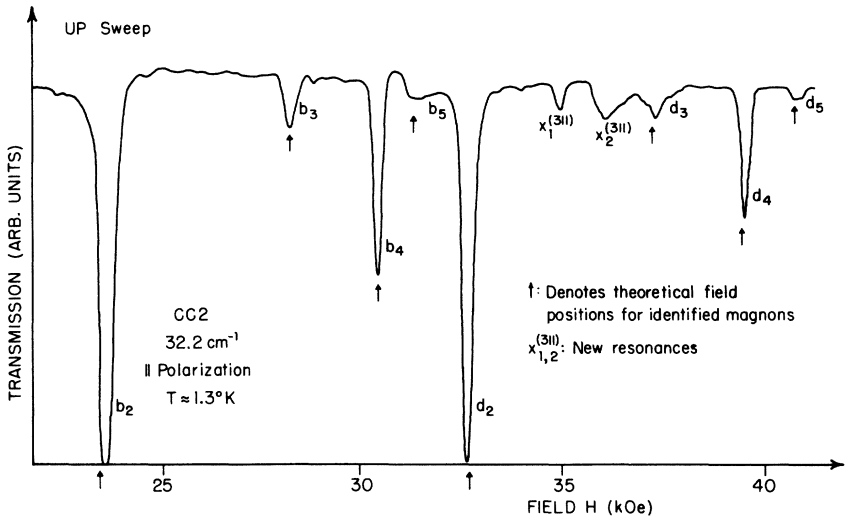

FIG. 5. Parallel polarization, 32.2-cm^{-1} laser transmission spectrum of CC2 at 1.3 °K which reveals two new resonances in the middle-field region — denoted $x_1^{(311)}$ and $x_2^{(311)}$.

+phonon resonance position to 59.0 ± 0.2 kOe observed experimentally confirms these model predictions. All other magnon positions were essentially unchanged in position from the ordinary CC2 case. The existence of this optic phonon is evidently not limited to CC2. Torrance and Slonczewski[26] have theoretically estimated the magnon-phonon coupling strength for the related linear-chain system $FeCl_2 \cdot 2H_2O$ (FC2; $S = 2$). The optical phonon observed by Hay and Torrance[27] in FC2 is nearly identical to that seen in CC2; the frequency E_{ph} is slightly higher and the coupling strength A_{ph} somewhat larger than for the cobalt system. It is also present in $CoBr_2 \cdot 2H_2O$.[28]

C. Spectroscopic evidence for domain structure

A number of weak resonances have been observed in the AF and Fi phases which cannot be accounted for by the basic theoretical spectrum of Fig. 1. A typical sweep of the middle-field region taken at 32.2 cm^{-1} with the even polarizer is shown in Fig. 5. There are two new resonances present, labeled $x_1^{(311)}$ and $x_2^{(311)}$ (32.2 cm$^{-1} \equiv 311$ μm). The expected field positions of the previously identified b_n and d_n are indicated on this sweep to illustrate the typical assignment agreements with experiment. The sample used was misaligned by a substantial angle, so that both cluster manifolds are clearly observed in a single sweep. At 29.7 cm^{-1} *three* new resonances are observed—one between b_4 and b_5, as well as ones on either side of d_2. It now appears that these resonances, plus additional new weak lines seen in the AF phase, owe their existence to the presence of *domain boundaries* in CC2, recently investigated by Motokawa.[29] We postulate the existence of additional Ising-like fans of lines in the E-vs-H spectrum, assuming the presence of these domain walls; there is some excellent quantitative agreement with observed spectra.

Motokawa has investigated the local spin orderings governed by exchanges J_1 and J_2 in the a-b plane; domain walls of arbitrary complexity necessarily must be composed of a combination of these basic spin configurations. There are eight "critical" fields H_{ci} (where the applied field H always points along the positive b axis) at which a central "down" chain is unstable with respect to spin flopping. One of these is the familiar Fi-Fo transition at H_{c2}. (The thermodynamic AF-Fi transition at H_{c1} is *not* such a local critical field.[30]) Critical fields H_{c3} and H_{c4}, which correspond, respectively, to cases I and II of Fig. 6, lie between H_{c1} and H_{c2}. Motokawa claims that only three of the remaining five local critical fields possible between $H = 0$ and $H = H_{c1}$ can exist in domain walls in CC2: H_{c5}, H_{c6}, and H_{c7}, corresponding, respectively, to cases III, IV, and V of Fig. 6. All these fields are summarized below; the two physically ambiguous fields are defined here as H_{c8} and H_{c9}:

$$H_{c2} \equiv (4J_1 + 2J_2)/g^{\parallel}\mu_B \cong 45.8 \text{ kOe}, \tag{5a}$$

$$H_{c3} \equiv (4J_1 - 2J_2)/g^{\parallel}\mu_B \cong 36.6 \text{ kOe}, \tag{5b}$$

$$H_{c4} \equiv (4J_1)/g^{\parallel}\mu_B \cong 41.2 \text{ kOe}, \tag{5c}$$

$$H_{c5} \equiv 0 \text{ kOe}, \tag{5d}$$

$$H_{c6} \equiv (2J_2)/g^{\parallel}\mu_B \cong 4.6 \text{ kOe}, \tag{5e}$$

$$H_{c7} \equiv (2J_1)/g^{\parallel}\mu_B \cong 20.6 \text{ kOe}, \tag{5f}$$

$$H_{c8} \equiv (2J_1 + 2J_2)/g^{\parallel}\mu_B \cong 25.2 \text{ kOe (physical?)}, \tag{5g}$$

$$H_{c9} \equiv (2J_1 - 2J_2)/g^{\parallel}\mu_B \cong 16.0 \text{ kOe (physical?)}. \tag{5h}$$

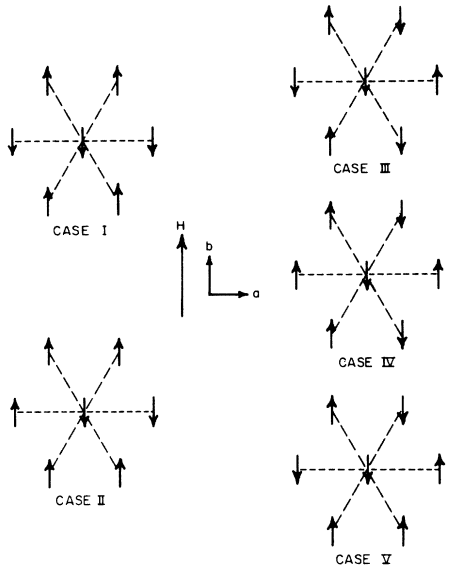

FIG. 6. Local-spin structures (Ref. 29) which produce critical fields between H_{c1} and H_{c2} (cases I and II), and below H_{c1} (cases III, IV and V).

The existence of fields H_{c3} and H_{c4} explains the weak additional ac susceptibility peaks found at 36.7 and 41.1 kOe by Kuramitsu *et al.*[31]; moreover, Motokawa[29] has observed the remaining two peaks at H_{c6} and H_{c7} ($H_{c5}=0$, unobservable). We proceed to investigate the implications for the E-vs-H spectrum. The Ising approximation is utilized for clarity; in reality, of course, the excitation fans are curved and split like those in Fig. 1.

We observe that *two* kinds of additional excitation fans become possible. The first kind represents spin clusters created on "down" chains (with the spin-flop critical fields H_{c2} through H_{c9}, above), with $dE/dH<0$. These are b_n or d_n like:

$$E^{(\downarrow)}_{i,n}\equiv 2J_0+ng^{\parallel}\mu_B(H_{ci}-H),\quad (H<H_{ci})$$
$$i=2,\ 3,\ \ldots,\ 9\ . \qquad (6)$$

However, a second category of excitations becomes possible: namely, spin clusters created on "up" chains, for which there are *no* spin-flop transitions ("critical" fields). Here, $dE/dH>0$, and one expects excitation fans which are c_n or e_n like:

$$E^{(\uparrow)}_{i,n}\equiv 2J_0+ng^{\parallel}\mu_B(H-H_{ci}),\quad (H>H_{ci})$$
$$i=2,\ 3,\ \ldots,\ 9\ , \qquad (7a)$$

and also those (like a_n) with *negative* field origins,

$$E^{(\uparrow)}_{-i,n}\equiv 2J_0+ng^{\parallel}\mu_B[H-(-H_{ci})],\quad (\text{all } H>0)$$
$$i=2,\ 3,\ \ldots,\ 9\ . \qquad (7b)$$

We now summarize the agreement with the data. For the spin environments associated with fields $\pm H_{c2}$, the only new excitations expected are of type (7b), but no HCN laser intersections are possible. Associated with $+H_{c3}$, Eq. (6) yields fan b_n *persisting* beyond H_{c1}, even though the crystal has nominally switched to the Fi phase. (The AF-Fi transition is known to be very hysteretic.[30]) Persisting b_4 and b_5 are seen clearly at 29.7 cm^{-1}. No evidence of fan (7a) has been found, and no HCN intersections result from the a_n extension produced by (7b). With critical field H_{c4} there is a d_n-like fan, which we call d'_n, whose excitations are seen added to the basic E vs H spectrum in Fig. 7. Table I shows the agreement with theory for magnons d'_2, d'_3, and d'_4; the new resonances in Fig. 5 are thus explained. There are no (7a)-type resonances observed, and none of kind (7b) possible at 30 cm^{-1}.

Associated with $\pm H_{c5}$ there is the extension of the ordinary c_n fan back into the AF phase. Magnon "c_1" has been clearly observed with odd polarization; its location (21 kOe) at 29.7 cm^{-1} agrees with the expected hybridization with the optic phonon. It typically possesses 0.1 to 1% of the b_1 + phonon intensity, indicating a surprisingly large domain wall volume for CC2. Similar intensities are found for the other new resonances. Magnon "c_2" has also been observed, at much reduced intensity. Fan (6) associated with H_{c6} yields HCN laser intersections with the vanishingly weak large-n clusters only; no structure is observed. The $n=1$ cluster of fan (7b) merges with the Lorentzian skirt of the very intense b_1 + phonon, making positive identification difficult.

Spectrum (6) with H_{c7} yields no $n=1$ laser intersection; the $n=2$ magnon has evidently been observed very weakly. Again, there is no evidence of fan (7a), and no 30-cm^{-1} intersections of (7b) possible. Finally, no structure has been observed in the laser spectra to indicate the existence of local-spin environments associated with fields $\pm H_{c8}$ or $\pm H_{c9}$, supporting Motokawa's claims for CC2. It must be stressed that the complexity and volume of domain walls found will obviously depend on sample purity, homogeneity of applied field, uniformity of thermal sinking, and the nature of the cycling of the sample in both field and temperature. A thorough investigation of domain wall behavior in CC2 remains to be accomplished.

IV. LOW-TEMPERATURE LINE SHAPES AND INTENSITIES

A. Line shape mechanism

The spin-cluster transmission resonances have been observed to range in shape from quite symmetric and highly Lorentzian to considerably asymmetric. Understanding the line-shape mechanism immediately became essential given the capability

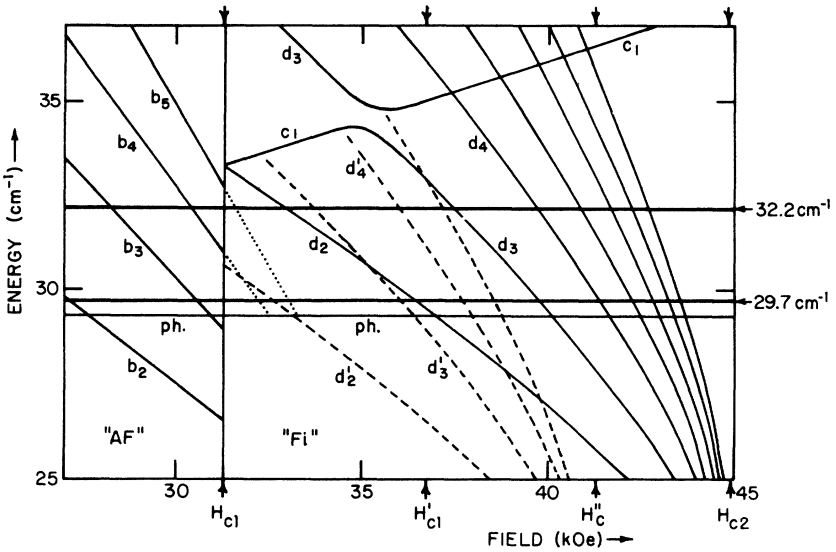

FIG. 7. Theoretical E-vs-H spectrum of CC2 in the middle-field region, including the proposed d'_n spin-cluster excitation "fan," with critical field at $H''_c = 41$ kOe.

to measure resonances widths to such high accuracy. A naive calculation of the effective attenuation coefficient based on a lossy dielectric with *incoherent* reflections at the sample surfaces yields

$$\alpha_{\text{eff}} \approx 4\pi \frac{\omega}{c} \sqrt{\epsilon'} \left(\chi''(\omega) + C\chi'(\omega) + \frac{1}{4\pi} \frac{\epsilon''}{\epsilon'} \right), \qquad (8)$$

$$(|4\pi\chi| \ll 1)$$

where

$$C \equiv \frac{1}{2} \frac{\epsilon''}{\epsilon'} + \frac{n_0 - 1}{n_0 + 1} \frac{1}{2\pi n_0} \frac{\lambda_{\text{laser}}}{d}, \qquad (9)$$

$$(n_0 \equiv \sqrt{\epsilon'}).$$

χ'' is presumably Lorentzian.

Rough estimates of the indices of refraction for the two polarizations were made at room temperature from direct reflection measurements:

$$n_{\text{odd}}(30\ \text{cm}^{-1}) \cong 1.90\text{–}1.95;$$

$$n_{\text{even}}(30\ \text{cm}^{-1}) \cong 2.35\text{–}2.50.$$

The value for n_{odd} was corroborated by a dc-limit measurement of the dielectric constant; hence, the value for n_{even} should also be reliable.

Measurements of the zero-field (nonresonant) transmission yielded an α of the order of 5/cm, or $\epsilon'' \cong 0.05$.

Accordingly, Eqs. (8) and (9) fail to describe the observed asymmetries. First, the most asymmetric resonances seen require 10 to 20% χ' admixture just to *approximate* the degree of skewing present; fraction C is 0.02–0.03 at most. Second, and more fundamentally, no unique sense of asymmetry is observed from sample to sample; the only consistency present is the obvious one owing to sign reversal of slope dE/dH—for a given frequency, polarization, and sample the asymmetries in field of the b_n's and d_n's are the mirror images of those of the e_n's (same n). Yet (8) implies a unique sense of skewing for *all* magnons having the same sign of dE/dH (all samples).

Instead, the asymmetries appear to be a consequence of "dimensional interference," discussed recently by Rado.[32] In the far infrared, unlike the microwave regime, a 1-mm crystal thickness represents up to 10 or more wavelengths; further-

TABLE I. Experimental and theoretical laser field intersections of selected spin clusters of the AF and Fi phases.

	Excitation	Expt. field (kOe)	Theor. field (kOe)
32.2 cm^{-1}	b_2	23.7	23.6
	b_3	28.3	28.2
	b_4	30.4	30.5
	b_5	31.5	31.6
	d_2	32.7	32.9
	d'_3	34.8	33.8
	d'_4	36.1	36.0
	d_3	37.4	37.5
	d_4	39.6	39.7
	d_5	40.8	40.9
29.7 cm^{-1}	b_2	27.4	27.2
	b_3	30.9	30.6
	b_4	31.9	32.1
	d'_2	32.5	32.6
	b_5	33.2	33.0
	d'_3	35.4	35.9
	d_2	36.5	36.4
	d'_4	38.0	37.7

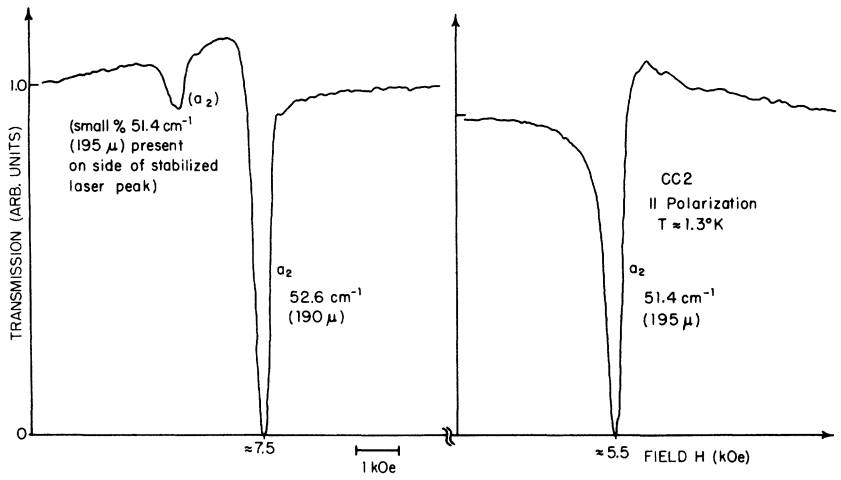

FIG. 8. Experimental qualitative verification of the interference-model origin of resonance asymmetries. Two opposite senses of skewness are observed for the same magnon, a_2, at the two DCN frequencies.

more, the laser radiation is highly monochromatic and the sample surfaces are very flat on the scale of the wavelength. Hence, the coherence of the waves in the medium must be considered. One can easily obtain the exact transmitted intensity ratio for a finite slab with permeability μ modulated by χ near resonance (Ref. 32).

One simply plots this function over the field range encompassing the resonance (represented by a Lorentzian of selected width and strength) to discover the shape of the transmission line shape expected for the "real" sample. The line shapes so generated are in excellent qualitative agreement with the observed spectra. The unusually large transmission "hump" (exceeding unity) is clearly reproduced for the more asymmetric lines. For a fixed frequency ν_{laser} and index n, the asymmetry is a very sensitive periodic function of crystal thickness L, with period $(c/\nu_{\text{laser}})(1/2n)$. Alternatively, for fixed ν_{laser} and thickness L_0, the asymmetry is periodic in the index n. A striking piece of experimental evidence in support of the interference mechanism is shown in Fig. 8. The resonance depicted is the two-cluster a_2 (AF) using both the 51.4- and 52.7-cm^{-1} DCN laser lines. For this particular sample the asymmetry completely *reversed* sense with a slight change in laser frequency!

The interference model line shape is so sensitive a function of frequency, index, and sample thickness that it was very difficult to assign parameter values so as to obtain consistent quantitative agreement with all the CC2 data. Nevertheless, it may be noted that for $L = 1.0$ mm and $n = 1.90$ (our estimate of n_{odd}) the model predicts nearly *identical* asymmetries at the two HCN frequencies for odd clusters. This is indeed found to be the case experimentally for the (nominal) 1.0-mm samples: e_{odd} are "steep left," and b_{odd} and d_{odd} "steep right," at *both* HCN frequencies. No such similar skewness is predicted or observed for the even-polarization case.

B. Low-T linewidths

The field widths at lowest temperature can be accurately measured only for the weaker magnons which are not "bottomed"—$n \geq 3$ for a 1-mm sample. The width is measured across the logarithmic half-power transmission points. The effects of interference skewing can be eliminated by resorting to computer-generated line shapes. Field widths are converted to energy widths using the Torrance-Tinkham dE/dH values at the laser crossings. The odd-cluster slopes at 29.7 cm^{-1} are lowered due to the strong optic phonon coupling (mediated by the basic $n = 1$ component). In the case of b_1 + phonon, the indicated slope is so small as to yield an energy width which appears to be anomalously small.

The $n = 3$ clusters in all three phases have widths of approximately 0.25–0.3 cm^{-1}. The widths of the strong $n = 1$, 2 clusters appear to range from slightly lower than this to as large as 0.4–0.5 cm^{-1} (see Sec. V). The widths of the higher-n clusters all grow uniformly to 0.5–0.6 cm^{-1} for $n = 5$, 7, and 8. This growth is partly due to merging effects as the spacings decrease (with the approach to critical field). Only 20–30% of the increase can be ascribed to field inhomogeneity, which has a greater effect the larger the slope. The variations in the width from sample to sample may be due to impurities and/or surface conditions (glue dissolving, straining, etc.). The over-all conclusion is that the linewidth increases somewhat with cluster size n, but is not significantly dependent on phase, frequency, or polarization (excluding the anomalous case of b_1 + phonon). In fact, the linewidth of a given size spin cluster increases *slightly* in going from the AF to Fi to Fo phases. The best example is that

of the $n=4$ cluster: in one sample the widths of b_4, d_4, and e_4 measured from a single sweep were approximately 0.28, 0.30, and 0.33 cm^{-1}, respectively. The width increases are evidently due to the progressive increase in magnetization of the sample from 0 to 100 to 300 G on going from the AF to Fi to Fo phases, respectively. The observed line broadening can be accounted for by assuming that the nonellipsoidal samples possess an inhomogeneity of internal field which is roughly 10% of the demagnetizing field in each case, a reasonable assumption for the typical sample dimensions employed. The small over-all *shifts* in resonance field positions associated with the mean values of the demagnetizing fields are unobservable in practice owing to absolute uncertainties in the values of H_{c1} and H_{c2}.

C. Relative and absolute intensities

We wish to calculate χ''; the $T=0$ case is chosen for simplicity:

$$\chi''_{ii}(\omega)=\frac{\pi}{\hbar}\sum_n |\langle\varphi_n|\mu^{(i)}|\varphi_0\rangle|^2\delta(\omega-\omega_{n0}), \qquad (10)$$

where $|\varphi_0\rangle$ denotes the ground state and $|\varphi_n\rangle$ represents the excited states of the system.

For a general spin-cluster excitation the computation of the matrix elements for (10) is in principle straightforward, given the diagonalization procedure for the single-chain Hamiltonian (3a). However, formal difficulties arise owing to the incompleteness of the basis. The set of states to be diagonalized should include the fully aligned chain $|0\rangle$ because of its coupling to $|2\rangle$ by $\mathcal{H}^a$. However, this coupling, unlike that between $|n\rangle$ and $|n+2\rangle$ for $n\neq 0$ [see (4)], *diverges* with the chain length N:

$$\langle 2|\mathcal{H}^a|0\rangle=-\sqrt{N}J_0^a. \qquad (11)$$

The implication is that the ground-state wave function $|\varphi_0\rangle$ is complicated, and *not* mostly $|0\rangle$ like, even though $J_0^a/J_0^{zz}\ll 1$. A large price is being paid formally for neglecting all higher "series" of Ising excitations in the diagonalization–states consisting of two or more *non*adjacent spin clusters. Only the lowest of these Ising-fan multiplets, "series I," was diagonalized by Torrance and Tinkham. These multiplets carry the basic exchange energy $M2J_0^{zz}$, where M is the number of distinct spin clusters for all excitations belonging to the series-M multiplet. State $|0\rangle$ is repelled downward in energy with the divergent factor $\sqrt{N}$ by the even manifold of the series I multiplet, but both manifolds of this first multiplet are similarly depressed with the *same* factor $\sqrt{N}$ relative to the respective manifolds of the higher lying series II multiplets. The final energy differences are of course all finite. Fogedby[33,34] has recently investigated the consequences of this J_0^a coupling between multiplets.

As an aside, we note that there should exist a small but measurable magnetization in the AF phase due to the even-cluster admixture in the ground state. When a small field is applied along the b axis, the amounts of even spin flip occurring in the a and b sublattices will differ ever so slightly; the admixture fraction is approximately equal to $2J_0^a/E_2$, where E_2 (a sublattice) increases with H, and E_2 (b sublattice) decreases with H. The resulting net magnetization is therefore not rigorously zero (except at $H=0$), but should be roughly equal to $M=2\times10^{-5}H$. [This assumes a decrease in the magnetization of a chain by $(2J_0^a/E_2)^2\times100\%=0.28\%$.] The low-field dc susceptibility of CC2 was measured using a Josephson junction rf superconducting-quantum-interference-device (SQUID) magnetometer. The magnetization was recorded using a sample-in–sample-out technique at a number of constant applied fields in the range 1–20 Oe and also as a function of temperature from 2.8 to about 12 °K. Unfortunately, the presence of a large paramagnetic susceptibility component ($\sim 1/T$) at lower temperatures plus the usual increasing parallel antiferromagnetic susceptibility at elevated temperatures prevented the determination of the small J_0^a-induced susceptibility. An upper bound could, however, be placed on the extent of the chain magnetization decrease–about twice the percentage quoted above.

Torrance and Tinkham avoided the divergent repulsion of state $|0\rangle$ by *excluding* the latter altogether from the basis set. The coupling between $|0\rangle$ and $|2\rangle$ was taken to be equal to $-2J_0^a$ as in the general case (4). The $|2\rangle$-state energy was then allowed to absorb the *entire* repulsion before diagonalization:

$$E_{|2\rangle}\to E_{|2\rangle}+|2J_0^a|^2/E_2^0. \qquad (12)$$

From that point on, the diagonalization is straightforward, if all that is desired is the set of lowest multiplet perturbed energies. The odd and even manifolds are kept strictly separated by $\mathcal{H}^a$.

When the limited single-manifold diagonalization is applied to the calculation of the intensity spectrum, the odd-polarization case is straightforward. If the $|1\rangle$ component of the eigenvector of the excited state in question is designated by $a_1^{(\mathrm{exc})}$, we have (for $h_{\mathrm{osc}}\parallel c$ axis),

$$\chi''_{cc}=\frac{1}{\Delta\omega}\frac{\pi}{\hbar}\frac{1}{4}\mu_B^2(g^{\infty})^2|a_1^{(\mathrm{exc})}|^2\frac{N}{V}. \qquad (13)$$

N/V is the linear-chain spin density, $\Delta\omega$ is the linewidth, and $g^{\infty}=2.72$ is the appropriate g factor.

Owing to the even-manifold coupling problem alluded to previously, we can only sketch the *approximate* value for even-polarization susceptibility (correct to within factors of 2 or so):

TABLE II. Intramanifold relative intensities at 32.2 cm^{-1}, Fo phase: theory ($\mathcal{H}$ diagonalization) vs experiment.

Magnon	Theor. intensity	Expt. total intensity
e_1	$\equiv 1.0$	0.6–0.9
e_3	0.18	$\equiv 0.18$[a]
e_5	0.066	0.07
e_7	0.031	0.03
e_2	$\equiv 1.0$	0.8–1.0
e_4	0.33	$\equiv 0.33$[a]
e_6	0.15	0.14
e_8	0.083	0.07

[a]Normalized to the theoretical value.

$$\chi''_{zz} = \frac{1}{\Delta\omega}\,\frac{\pi}{\hbar}\,\mu_B^2 (g^{zz})^2 \left|a_2^{(\mathrm{exc})}\right|^2 \beta^2 \frac{N}{V}, \quad (\beta \sim J_0^a/E_2^0). \tag{14}$$

$a_2^{(\mathrm{exc})}$ represents the $|2\rangle$ component of the eigenvector in question.

Table II contains the comparison between theoretical and experimental integrated intensities at 32.2 cm^{-1}—away from the phonon—for e_1, e_3, e_5, e_7 and e_2, e_4, e_6, e_8 (Fo phase). The e_1 and e_2 values were obtained from Lorentzian fits, as they were strongly bottomed; the others were more accurately determined. Hence, the intensities have been normalized to the good e_3 and e_4 values. The agreements are reasonably good. We remark that at 50 cm^{-1} the e_3 strength is already reduced to that of e_9 or e_{10} at 30 cm^{-1} owing to the larger level spacings.

We now compare the absolute experimental intensity of the basic e_1 excitation with the quantum-mechanical result, (13). The attenuation coefficient at resonance is usually employed [see (8)]: $\alpha(\omega_0) \approx 4\pi(\omega_0/c)\sqrt{\epsilon'}\,\chi''(\omega_0)$. For some purposes it is more useful to deal instead with the (normalized) Lorentzian susceptibility strength S_E, defined by $\chi''(\omega_0) = 2S_E/\pi\Gamma$, where Γ denotes the full energy width at half-intensity. Then,

$$S_E\big|_{|0\rangle\to|1\rangle} = \frac{\pi^2}{8}\,\mu_B^2 (g^{cc})^2 \frac{N}{V}, \quad \text{(theor.)} \tag{15}$$

$$S_E = \frac{\alpha(\omega_0)\Gamma}{8(\omega_0/c)\sqrt{\epsilon'}}, \quad \text{(expt.)} \tag{16}$$

Table III lists these values at 32.2 cm^{-1} for e_1 and also for e_3 and e_5. The two Lorentzian fits to bottomed e_1 indicate the rough degree of fitting uncertainty involved. (It would obviously be desirable to develop techniques for the fabrication of very thin samples, made difficult because CC2 is so brittle a material.) There is much closer agreement for e_3 and e_5, which can be accurately measured.

As regards the even-cluster absolute intensities we simply record the experimental intensity of the most accurately measured resonance, e_4, at 32.2 cm^{-1}:

$$\alpha(E_0) \cong 9.2 \text{ (per cm)}, \quad (\Gamma \cong 0.37\ cm^{-1}),$$

$$S_E \cong 0.85\times10^{-3}\ cm^{-1}.$$

All other e_{even} intensities are related theoretically to the above by the $\mathcal{H}$ diagonalization, via (14) (and Table II). The purpose in presenting these absolute intensities for comparison is to provide the stimulus for calculation of the even-odd-manifold problem.

V. TEMPERATURE DEPENDENCE OF SPECTRUM

A. Linewidths

One of the most interesting, and least understood, aspects of the CC2 excitation spectrum was revealed when field sweeping was performed at elevated temperatures, up to about 15 °K. Figure 9 shows representative sweeps at 29.7 cm^{-1} of the e_{even} made at a number of fixed temperatures. Not shown in Fig. 9 are data taken at $T > 10$ °K, at which point the resonances all acquire additional "artificial" broadening and substantial skewing due to the superposition of the skirts of the broadened adjacent resonances. In the case of the e_n's, the line shapes in field are all "pulled" in the direction of decreasing field, while for the b_n's and d_n's the skewing is in the opposite direction. In practice, therefore, 13 or 14 °K represents the highest temperature at which one can reasonably confidently adjust the apparent widths for this merging effect, even though the resonances remain quite "visible" at higher temperatures (for e_1, almost to $T_N \approx 17$ °K).

The data divide quite naturally into two categories: With 1-mm-thick crystals the $n = 1$, 2 clusters are sufficiently strong that they "bottom" to zero at low temperatures; only at 8–9 °K have they lifted, permitting accurate width determinations out to about 14 °K. In the second category, $n \geq 3$, the low-T widths are determined easily enough, but these weaker lines become too spread out for effective measurement beyond about 9 °K. One finds for both categories that the full energy width Γ increases only slightly from 1.3 to between 3.0

TABLE III. Absolute intensities of resonances e_1, e_3, e_5: theory vs experiment.

	$\alpha(E_0)$ (per cm)		S_E (cm^{-1})	
Magnon	Theor.	Expt.	Theor.	Expt.
e_1 (fit No. 1)	420	115	3.6×10^{-2}	0.96×10^{-2}
e_1 (fit No. 2)	420	144	3.6×10^{-2}	1.20×10^{-2}
e_3	69	44	6.3×10^{-3}	4.0×10^{-3}
e_5	23	17	2.4×10^{-3}	1.9×10^{-3}

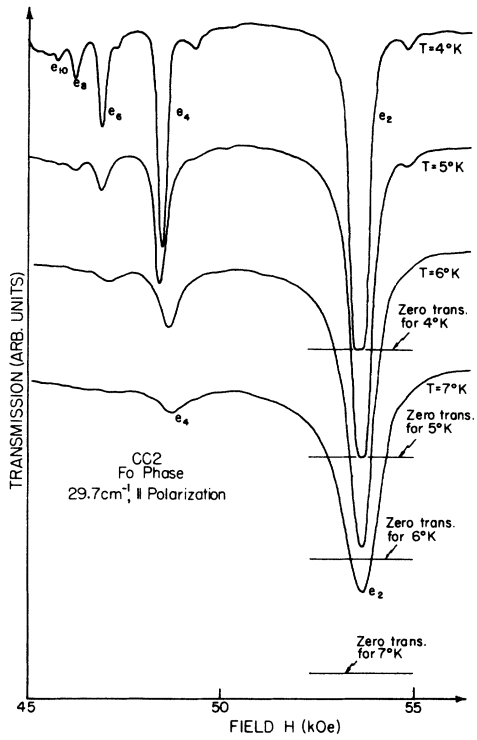

FIG. 9. Representative parallel polarization 29.7-cm^{-1} laser transmission spectra of CC2 in the Fo phase taken at several temperatures between 4 and 7 °K.

and 4.0 °K, depending on the resonance. This low-T width we designate by Γ_0. Beyond about 4.0 °K the widths all begin to increase dramatically with T. The dE/dH slopes at low temperature (determined from Fig. 1) are assumed in calculating the energy widths at all temperatures. The general experimental finding is that those resonances which can be observed over some substantial temperature range (viz. $n \leq 3$) obey a simple exponential broadening law (for $T \gtrsim 2\Gamma_0$),

$$\Gamma(T) \approx \Gamma_0 + Ae^{-\Delta/kT}, \qquad (17)$$

where a universal value for Δ is obtained [≈ 30 cm^{-1} (± 3 cm^{-1})]. This functional form was obtained not only for the 29.7- and 32.2-cm^{-1} magnon intersections but also for e_2 at 52.7 cm^{-1}. (e_1 was inaccessible with the 125-kOe maximum field with DCN radiation.) It holds as well for the phonon-admixed spin-wave b_1 + phonon, even though the energy widths are anomalously small if one assumes the very small dE/dH at 29.7 cm^{-1}. Figure 10 illustrates a typical fit for b_2. Unfortunately, the merging problems for the $n \geq 4$ clusters are so severe at the HCN frequencies that only very short temperature sequences (e.g., 3 to 6 °K) can be obtained for these resonances before they effectively disappear. The approach adopted for $n \geq 4$ was to assume (17), with a Δ of 30 cm^{-1}, and let the few data points determine parameters Γ_0 and A. The results are summarized in Table IV.

Γ_0 is found to vary between about 0.2 and 0.6 cm^{-1}, with no obvious correlation to cluster size, phase, or exciting frequency. Much of the variation appears to be sample related, probably depending on inclusions, domaining, glue dissolving, etc. Prefactor A is the more interesting parameter. It ranges from about 35 cm^{-1} for the $n = 1$ cluster to well over 1000 cm^{-1} for the largest of the spin clusters, *if* one believes that fit (17) is applicable to the latter. A increases dramatically, then, with increasing cluster size n. In addition, it appears to decrease with increasing excitation frequency, following the dependence, $A \sim 1/\nu^2$ (n.b., there are only three frequencies available for comparison, with a limited amount of data recorded at each one).

A striking feature of the exponential fit is that the universal value found for Δ happens to coincide with a characteristic energy of the CC2 system–the optic phonon energy $E_{ph} \cong 29.3$ cm^{-1}. Now, the Δ found holds for both odd- and even-size clusters, even though only the former show admixture to the optic phonon in the low-T E-vs-H spectrum (Fig. 1). The single-chain spin Hamiltonian (3a) clearly does not allow communication between the odd and even manifolds. The DCN laser data on e_2 in the vicinity of 50 cm^{-1} show the *same* Δ, demonstrat-

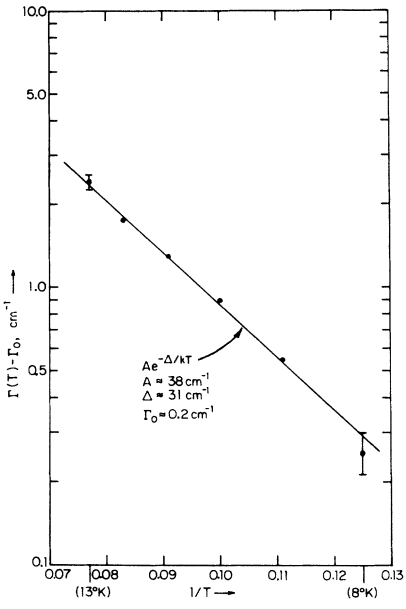

FIG. 10. Exponential fit to the temperature-dependent linewidth $\Gamma(T)$ of resonance b_2 measured at 29.7 cm^{-1}: $\Gamma(T) - \Gamma_0$ vs $1/T$ for 8 to 13 °K, where the low-T width Γ_0 is approximately 0.2 cm^{-1}. A universal value for Δ, approximately 30 cm^{-1}, has been obtained for all resonances measured.

TABLE IV. Values of Γ_0 and A found for the exponential linewidth fits, $\Gamma(T) = \Gamma_0 + Ae^{-\Delta/kT}$ ($\Delta = 30$ cm^{-1}).

Spin cluster	Laser freq. (cm^{-1})	Γ_0 (cm^{-1})	A (cm^{-1})
e_1	32.2	0.5–0.6	65
e_2	29.7	0.2–0.3	140
	32.2	0.2	120
	52.7	0.2	50
e_3	32.2	0.3	380
e_4	29.7	0.3–0.4	1020
	32.2	0.4	850
e_5	32.2	0.3–0.4	2100
b_1 + phonon	29.7	0.1[a]	10[a]
b_2	29.7	0.2	38
	32.2	0.1	33
b_3	32.2	0.3	85

[a]Anomalously small owing to the very small dE/dH assumed at the laser line crossing, a consequence of the strong optic phonon coupling at approximately 30 cm^{-1}.

ing that the exciting energy does not determine Δ; hence, the simple mechanism of *direct* phonon absorption-emission is ruled out.

It appears that the linewidth temperature dependence may be explained, at least qualitatively, by the presence of *continua* of excited states in the higher Ising multiplets due to J_0^a. (That is, the upper Ising fans are not discrete.) Hence, at finite T absorption can occur between smeared-out higher levels—effectively yielding a broadened line without the need for a relaxation mechanism *per se*. One encouraging feature of this model, advanced by Fogedby,[35] is that the linewidth at a given temperature is predicted to increase dramatically the closer one is to the Ising-fan origin—i.e., the larger is n for a fixed laser frequency. This is indeed the observed behavior of prefactor A.

There remains a rather surprising feature of the T-dependent spectrum: As T increases the resonances broaden considerably, but their (peak) field positions hardly vary at all, all the way to 13 or 14 °K. This behavior is surprising, given the expression for the simple Ising spectrum,

$$E_n = 2J_0 \pm ng^{\parallel}\mu_B(H - H_{\rm crit}), \tag{18}$$

because one presumes that $H_{\rm crit}$ should be replaced by $H_{\rm crit}(T)$ at elevated temperatures. The H-T phase diagram expected[11,12,36] for CC2 is that given approximately in Fig. 11. The laser spectroscopy technique, in fact, is able to directly measure $H_{c2}(T)$ [but *not* $H_{c1}(T)$] over a substantial part of its range owing to the sharp step, or "heel," in transmission occurring at the d_n/e_n interface. (The e_n's absorb more than the corresponding d_n's because of the threefold greater sublattice percentage.) This step travels downward in field with increasing T, although it loses sharpness at higher-temperatures due to cluster broadening. The authors' limited data ($T \leq 8$ °K) are indicated in Fig. 11. $H_{c2}(T)$ at 13 or 14 °K is seen to be many kOe reduced from the 45-kOe $T = 0$ value. Clearly, then, the spin-cluster resonances have their peak field positions determined by the "local," low-T critical field, rather than by the average, or T-dependent, value. Such a result casts light again on the highly localized nature of these cluster resonances.

B. Integrated intensities

For the $n = 3$ clusters b_3 and e_3 measured at 32.2 cm^{-1}, the integrated intensity $I(T)$ is found to be very nearly constant over the entire measurable range, 1.3 to 8 °K (~5% random scatter in measured values). For the stronger $n = 1$, 2 clusters the total intensities are nearly constant up to about 7–8 °K and then begin a smooth decline.

One can make a simple but rather convincing theoretical model for the temperature dependence of $I(T)$ based on the Ising model, using quantities developed by Date and Motokawa.[15–17] In the localized spin-flip language, as T increases there are fewer up segments of aligned spins available on the thermally agitated chains to support spin-cluster creation. Date and Motokawa made use of the quantities n_s/N and n_c/N for an Ising loop of N spins at field H_0 and temperature T. These are, respectively, the (N-normalized) total number of spins pointed down and the total number of clusters (see Ref. 16 for formulas).

The Torrance-Tinkham values, $J_0^{zz}/k = 18.2$ °K and $g^{zz} = 6.8$, were used to compute these parameters for various H_0 and T values. The reader should note this important difference from the Date and Motokawa work—the spectroscopically determined J_0 is about *twice* the value determined indirectly in the early work on CC2 (discussed below). Consequently, at a given H_0 and T both n_s/N and

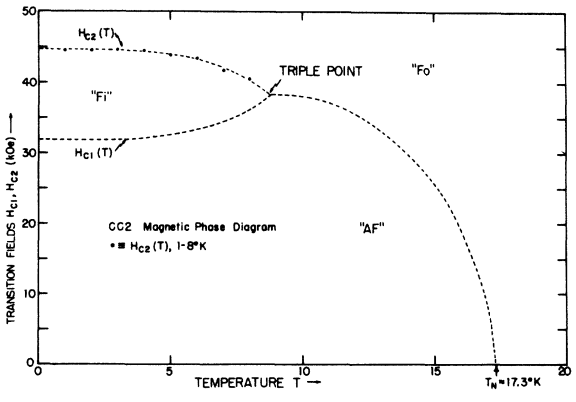

FIG. 11. Schematic plot of the H-T magnetic phase diagram for CC2 obtained from mean-field calculations. The points show the authors' data for $H_{c2}(T)$ over a limited temperature range.

n_c/N are considerably smaller than the corresponding values found in Ref. 16.

In an aside we note that the early indirect estimate of J_0 alluded to above consisted of a molecular-field calculation of the Néel temperature T_N (see Refs. 9, 11, and 12). The value obtained for T_N depended on J_0 and the interchain exchanges J_1 and J_2. T_N was estimated to be 17.2 °K from the specific-heat anomaly, and J_1 and J_2 were determined from transition fields H_{c1} and H_{c2}. Hence, an estimate for J_0/k was obtained: 9.3 °K. However, a more refined calculation is needed to produce a convincing value for J_0—one which squares with the value determined by far-infrared spectroscopy. It should be noted that the H-T phase diagram (Fig. 11) experimentally verified by Lowe *et al.*[36] recently and determined originally by Yamada and Kanamori finds agreement for the triple point location and the T_N value using the molecular-field value of J_0/k. Nevertheless, if one sets the interchain exchanges equal to zero, these models predict an ordering of the system—whereas, rigorously, a linear-chain model does not order at *any* field at finite T. The Appendix contains two very approximate model calculations of T_N which support the 18 °K choice for J_0/k.

Considering a single Ising chain, we can arrive at a crude measure of spin-cluster intensity: the fraction of the chain which is still "up,"

$$I(H_0,\ T) \approx (N - n_s)/N = 1 - n_s/N . \tag{19}$$

However, one can do better than this. On the thermally agitated chain only those up segments which are of size $n+2$ or larger are capable of supporting the creation of an n cluster. If the size of the up segment is p spins, then there are $p-n-1$ ways of creating the n cluster in the localized picture. The correct normalization results from dividing the total count by N, the number of available ways at $T=0$ (assume $N \to \infty$). Letting $N'(p;\ H_0,\ T)$ denote the (mean) number of up segments of size p (field H_0, temperature T), we expect that the normalized intensity of an n-cluster excitation should be

$$I_n(H_0,\ T) = \frac{1}{N} \sum_{p \geq n+2}^{N} N'(p;\ H_0,\ T)(p - n - 1) . \tag{20}$$

Date and Motokawa[16] used combinatorial techniques to determine the number of thermally created spin clusters of size p, called $n_{e,\,m=p}$,

$$n_{e,\,m=p} \approx (n_c^2/n_s)(1 - n_c/n_s)^{p-1} \quad (n_c,\ n_s \gg 1) . \tag{21}$$

The above refers to the distribution of n_s *down* spins among the n_c (down) clusters. Adapting it to the calculation of $N'(p;\ H_0,\ T)$ requires only the substitution, $n_s \to N - n_s$ (and trivially, $n_c \to n_c$). Thus, we have

$$N'(p;\ H_0,\ T) \cong \frac{n_c^2}{N - n_s} \left(1 - \frac{n_c}{N - n_s}\right)^{p-1} \quad (n_c,\ n_s \gg 1) . \tag{22}$$

The intensity becomes

$$I_n(H_0,\ T) \approx \frac{n_c}{N}(1 - x)\left(\sum_{p \geq n+2}^{N} p x^{p-1} - 2 \sum_{p \geq n+2}^{N} x^{p-1} \right) , \tag{23}$$

where

$$x \equiv 1 - (n_c/N)/(1 - n_s/N) . \tag{24}$$

Performing the discrete summations in the limit $N \to \infty$, we find,

$$I_n(H_0,\ T) = (1 - n_s/N) x^{n+1} . \tag{25}$$

Figure 12 shows the agreement for e_1, CC2D, at 29.7 cm^{-1}. The low-T value for H_{c2} has been assumed, so that $H_0 = H(29.7\ cm^{-1},\ e_1) - H_{c2}(T=0)$ = 15 kOe. The agreement is seen to be quite reasonable. (The error brackets are due primarily to merging correction uncertainties.) Another convincing test is afforded by the e_2 data at 52.7 cm^{-1}. Field H_0 is about 43 kOe, again assuming the low-T value for H_{c2}. At 13 °K one obtains a theoretical intensity of 0.95; the experimental measurement is 0.91 ± 0.04.

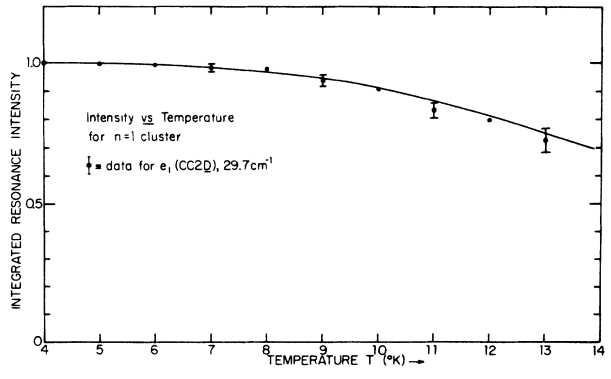

FIG. 12. Ising model prediction of the T dependence of the $n=1$ spin-cluster integrated intensity, compared to the experimental values for resonance e_1, 29.7 cm^{-1}, $CoCl_2 \cdot 2D_2O$. Only representative error bars are shown.

VI. SUMMARY AND CONCLUSIONS

The far-infrared transmission spectroscopy of $CoCl_2 \cdot 2H_2O$, first carried out in detail by Torrance and Tinkham, has been extended in the present work with the aid of a stabilized HCN/DCN laser. Qualitative, as well as quantitative, improvements in the measured "multiple-magnon" spectrum of this nearly Ising linear-chain system have resulted. Spin clusters of up to 14 adjacent flipped spins were clearly observed, as well as very weak resonances which corroborate the existence of numerous domain walls recently postulated by Motokawa.

Laser spectroscopy has permitted the detailed investigation of the temperature dependence of the spin-cluster linewidths and intensities. There is good agreement of the low-temperature intensities with the quantum mechanics of the general single-chain exchange Hamiltonian; the temperature dependence of the intensities agrees well with the statistics of the linear Ising model. For the stronger resonances the dramatic increase in linewidth with temperature is found to closely follow a universal exponential law. The characteristic energy of the latter suggests that the optic phonon in the system may be implicated in the relaxation of the spin clusters.

Approximate calculations of T_N are given to show that the large value of interchain exchange J_0 found spectroscopically by Torrance and Tinkham and corroborated by our temperature-dependent intensity calculations is also consistent with the observed T_N. This value of J_0 is twice that found by a number of authors by estimates using mean-field models. A fascinating result was obtained from the temperature-dependent spectra; namely, as the resonances broaden with increasing temperature, their field positions (i.e., the laser intersections) do *not* move substantially. This behavior is strange, given that transition fields H_{c1} and H_{c2}—regarded as the "origins" of the various Ising fans—are known from the magnetic phase diagram to shift drastically at elevated temperatures. This behavior emphasizes again the highly localized nature of the spin-cluster excitations seen in this unusual magnetic insulator.

ACKNOWLEDGMENTS

We would like to thank Hans C. Fogedby for many useful discussions regarding the theoretical interpretation of these experiments, and J. B. Torrance and John Peech for valuable experimental suggestions in the initial stages of this work. One of us (D. F. N.) also wishes to thank the National Science Foundation for providing him with a Graduate Fellowship during his enrollment at Harvard University.

APPENDIX

The results of two greatly simplified calculations applied to CC2 will be discussed, in an attempt to relate the Néel temperature to J_0, J_1, and J_2. They can be regarded as alternatives to the standard mean-field approximations, which require the small value for J_0/k of about 9 °K.

First, we consider the well-known Bethe-Peierls model, which accounts for nearest-neighbor spins exactly, with further neighbors lumped into a mean field. It yields a critical temperature T_N given by

$$kT_N = J/\ln[\gamma/(\gamma-2)], \tag{A1}$$

where exchange J agrees with the authors' convention. Parameter γ is the coordination number—the number of nearest neighbors of a given spin, coupled by J. The ordinary linear Ising chain case, $\gamma = 2$, yields $T_N = 0$, which happens to be rigorously correct. Applying (A1) to CC2, one can try to account for the differing J_1 and J_2 (which induce ordering at finite T) by fabricating an "effective" γ,

$$\gamma_{\text{eff}} = 2 + 4\left|J_1^{zz}/J_0^{zz}\right| + 2\left|J_2^{zz}/J_0^{zz}\right|. \tag{A2}$$

The two intrachain neighbors are clearly the most important because of the very large J_0^{zz} value. The idea behind (A2) is that the four J_1 neighbors and two J_2 neighbors should also be counted in γ (generalized to be nonintegral), but with *reduced* effectiveness—in proportion to their respective smaller exchange with the "central" spin. The resulting γ_{eff} of 3.1 combined with our spectroscopically measured J_0^{zz}/k of 18.2 °K produces

$$T_N \text{ (modified "Bethe-Peierls")} \cong 17.5\ ^\circ\text{K},$$

surprisingly close to the accepted T_N of 17.2 °K!

A second very approximate approach is to use the *exact* result for T_N for the two-dimensional Ising net with exchanges J and J':

$$\sinh(J/kT_N)\sinh(J'/kT_N) = 1. \tag{A3}$$

For J we use the large J_0^{zz}. For J', an effective value is fabricated:

$$J' = 2J_1 + J_2.$$

Solving (A3) for T_N, we find

$$T_N \text{ (two-dimensional Ising net)} \cong 15.8\ ^\circ\text{K}.$$

The agreement with experiment is again reasonable. The spirit behind these approximate calculations has been to recognize that the disproportionately large exchange J_0 is really *the most* important coupling in CC2. Hence, one should be able to deal with the much smaller interchain exchanges in an approximate way, with their effects diminished roughly in proportion to their size relative to J_0. While no claim is made as to the accuracy of these calculations, the authors would nevertheless argue that the results are more quantitatively reliable than those of a molecular-field model. A careful calculation of the full exchange-coupling problem which retains more of the integrity of the special Ising chains should be carried out to lay to rest this exchange constant controversy.

---

†Work supported in part by the National Science Foundation, the Office of Naval Research, and the Advanced Research Projects Agency.

*Present address: Physics Department and Center for

Materials Science, Massachusetts Institute of Technology, Cambridge, Mass. 02139.

[1]A. Narath, Phys. Rev. 136, A766 (1964).
[2]A. Narath, J. Phys. Soc. Jap. 19, 2244 (1964).
[3]A. Narath, Phys. Lett. 13, 12 (1964).
[4]A. Narath, Phys. Rev. 140, A552 (1965).
[5]D. E. Cox, B. C. Frazer, and G. Shirane, Phys. Lett. 17, 103 (1965).
[6]I. F. Silvera, Ph.D. thesis (University of California, Berkeley, Calif., 1965) (unpublished).
[7]H. Kobayashi and T. Haseda, J. Phys. Soc. Jap. 19, 765 (1964).
[8]T. Oguchi and F. Takano, J. Phys. Soc. Jap. 19, 1265 (1964).
[9]T. Shinoda, H. Chihara, and S. Seki, J. Phys. Soc. Jap. 19, 1637 (1964).
[10]T. Ogushi, J. Phys. Soc. Jap. 20, 2236 (1965).
[11]K. Yamada and J. Kanamori, Progr. Theoret. Phys. 38, 541 (1967).
[12]J. Kanamori, Progr. Theoret. Phys. 35, 16 (1966).
[13]A. Narath and J. E. Shirber, J. Appl. Phys. 37, 1124 (1966).
[14]D. E. Cox, G. Shirane, B. C. Frazer, and A. Narath, J. Appl. Phys. 37, 1126 (1966).
[15]M. Date and M. Motokawa, Phys. Rev. Lett. 16, 1111 (1966).
[16]M. Date and M. Motokawa, J. Phys. Soc. Jap. 24, 41 (1968).
[17]M. Date and M. Motokawa, J. Appl. Phys. 39, 820 (1968).
[18]J. B. Torrance, Jr. and M. Tinkham, J. Appl. Phys. 39, 822 (1968).
[19]J. B. Torrance, Jr. and M. Tinkham, Phys. Rev. 187, 587 (1969).
[20]J. B. Torrance, Jr. and M. Tinkham, Phys. Rev. 187, 595 (1969).
[21]J. B. Torrance, Jr., Ph.D. thesis (Harvard University, Cambridge, Mass., 1969) (unpublished).
[22]D. F. Nicoli, Ph.D. thesis (Physics Department, Harvard University, Cambridge, Mass., 1972) (unpublished).
[23]D. F. Nicoli, Tech. Rept. No. 5 (Harvard University, Cambridge, Mass., 1973) (unpublished).
[24]D. F. Nicoli and M. Tinkham, AIP Conf. Proc. 10, 1699 (1972).
[25]D. F. Nicoli (unpublished).
[26]J. B. Torrance and J. L. Slonczewski, Phys. Rev. B 5, 4648 (1972).
[27]K. A. Hay and J. B. Torrance, Jr., Phys. Rev. B 2, 746 (1970).
[28]J. B. Torrance and K. A. Hay, in Ref. 24.
[29]M. Motokawa, J. Phys. Soc. Jap. (to be published).
[30]M. Tinkham, Phys. Rev. 188, 967 (1969).
[31]Y. Kuramitsu, K. Amaya, and T. Haseda, J. Phys. Soc. Jap. 33, 83 (1972).
[32]G. T. Rado, Phys. Rev. B 5, 1021 (1972).
[33]Hans C. Fogedby and H. Højgaard Jensen, Phys. Rev. B 6, 3444 (1972).
[34]Hans C. Fogedby (unpublished).
[35]Unpublished calculation of Hans C. Fogedby.
[36]M. A. Lowe, C. R. Abeledo, and A. A. Misetich, Phys. Lett. 37A, 274 (1971).